Effects of two-step homogenization on precipitation behavior of Al_3Zr dispersoids and recrystallization resistance in 7150 aluminum alloy

Zhanying Guo [1,2], Gang Zhao [2], X.-Grant Chen [1,*]

[1] Department of Applied Science, University of Québec at Chicoutimi,
Saguenay (QC), Canada G7H 2B1
[2] Key Laboratory for Anisotropy and Texture of Materials,
Northeastern University, Shenyang, China, 110819

Abstract

The effect of two-step homogenization treatments on the precipitation behavior of Al_3Zr dispersoids was investigated by transmission electron microscopy (TEM) in 7150 alloys. Two-step treatments with the first step in the temperature range of 300–400 ˚C followed by the second step at 470 ˚C were applied during homogenization. Compared with the conventional one-step homogenization, both a finer particle size and a higher number density of Al_3Zr dispersoids were obtained with two-step homogenization treatments. The most effective dispersoid distribution was attained using the first step held at 300 ˚C. In addition, the two-step homogenization minimized the precipitate-free zones and greatly increased the number density of dispersoids near dendrite grain boundaries. The effect of two-step homogenization on recrystallization resistance of 7150 alloys with different Zr contents was quantitatively analyzed using the electron backscattered diffraction (EBSD) technique. It was found that the improved dispersoid distribution through the two-step treatment can effectively inhibit the recrystallization process during the post-deformation annealing for 7150 alloys containing 0.04-0.09 wt% Zr, resulting in a remarkable reduction of the volume fraction and grain size of recrystallization grains.

Keywords: 7150 aluminum alloy, Al_3Zr dispersoids, Two-step homogenization, Recrystallization

* Corresponding author: X.-Grant Chen

Department of Applied Science, University of Québec at Chicoutimi
Saguenay (QC), Canada G7H 2B1
Tel.: 1-418-545 5011 ext. 2603; Fax: 1-418-545 5012
E-mail: xgrant_chen@uqac.ca

1. Introduction

7xxx series aluminum alloys have high strength to density ratio and excellent mechanical properties, such as high strength, high fracture toughness and good resistance to stress corrosion, and are widely used in the aeronautical and astronautic industries [1-4]. However, recrystallization can significantly deteriorate mechanical properties of heat-treated materials; moreover, the fracture toughness of 7xxx alloys decreases with the increase of the recrystallization degree that occurs during the hot-forming process and solution heat treatment [4].

Small quantities of Zr are commonly added into 7xxx Al alloys as a recrystallization inhibitor, in which thermally stable Al_3Zr dispersoids precipitate during the homogenization of cast ingots. Al alloys with Zr additions can retain their deformed structure and prevent recrystallization, due to the presence of Al_3Zr dispersoids, even when annealed at high temperature [5]. The effectiveness of Al_3Zr dispersoids strongly depends on their size, number density and distribution [6]. It is recognized that Zr tends to segregate and enrich in the dendrite centers during solidification [7-9]. It is difficult to remove Zr concentration gradients during conventional homogenization due to Zr's low diffusivity in Al [10, 11]. Therefore, the precipitation of Al_3Zr dispersoids often concentrates in the center of dendrite gains and the precipitate free zone (PFZ) of dispersoids forms in dendrite grain boundaries [12-14].

The effects of both the Zr content and the homogenization condition on the precipitation of Al_3Zr dispersoids and the recrystallization of Al alloys have been investigated in previous studies [14, 16-20]. The conventional homogenization treatment (one-step) is mainly intended to dissolve low melting eutectic phases and to redistribute the solutes in aluminum matrix, but not necessary to optimize the precipitation of Al_3Zr dispersoids. The high homogenization temperature of the conventional practice causes both high solubility and diffusion rate of zirconium, which results in a low volume fraction of large dispersoids and wide precipitate free zones. To improve the distribution of Al_3Zr dispersoids, some approaches to stepwise homogenization were explored in the literature [12, 19, 20-22]. The first step was used to create a

favorable condition of dispersoid precipitation for developing an optimized distribution. The subsequent step then completed the homogenization of the alloy in the conventional manner. However, the nucleation, growth and distribution of dispersoids during the homogenization process are not well understood and the related recrystallization behavior of deformed materials was not quantitatively examined.

In the present study, the effects of one-step and various two-step homogenization treatments on the precipitation behavior of Al_3Zr dispersoids in the 7150 alloy were investigated. Particular attention was paid to the formation of Al_3Zr dispersoids during the first step of homogenization, which was designed to promote the nucleation of dispersoids and thus to improve the overall distribution of Al_3Zr dispersoids in the final homogenization step. The influence of two-step homogenization conditions on the recrystallization resistance of 7150 alloys with varying Zr content was quantitatively analyzed during the post-deformation annealing.

2. Experimental procedure

Four experimental alloys with different Zr contents were prepared by the ingot metallurgical route. The alloys were melted and batched in a graphite crucible using an electrical resistance furnace. The melt was poured at a temperature of 750 ˚C into a rectangular permanent steel mold to produce cast ingots measuring 30 x 40 x 80 mm^3. The chemical compositions of the experimental alloys are listed in Table 1 (all compositions are in wt% unless otherwise indicated). The homogenization processes included both conventional homogenization (one-step) where samples were held at 470 ˚C for 24 h and the new two-step homogenization treatments. For the two-step homogenization, two temperatures (300 ˚C and 400 ˚C) and two holding times (48 h and 72 h) were used in the first step of treatment, while the second step was the same as the one-step homogenization. After the completion of the homogenization treatment, the samples were subjected to direct water quenching. To study the effect of each step of homogenization on the dispersoid precipitation, some selected samples after the first step of treatment were also water-quenched. The details of both the one-step and two-step homogenization treatments are

provided in Table 2.

Cylindrical compression samples 10 mm in diameter and 15 mm in height were machined from the homogenized samples. Uniaxial hot compression tests were performed on a Gleeble 3800 thermomechanical simulator at a deformation temperature of 400 ˚C with a constant strain rate of 1 s^{-1}. Compression samples were deformed to a total true strain of 0.8 and subsequently water-quenched. To evaluate the recrystallization resistance after the post-deformation heat treatment, the deformed samples were annealed at 470 ˚C for 2 h, followed by water quenching to room temperature.

To study the precipitation of Al_3Zr dispersoids, the homogenized samples were examined under a transmission electron microscope (TEM, JEOL JEM-2100) operated at 200 kV. TEM specimens were mechanically ground to approximately 40-μm thickness, followed by twin-jet electropolishing at 15 V DC in a 30% nitric acid and 70% methanol solution cooled to -25 ˚C. The TEM examination was performed with the specimen oriented along low index [011] zone axis of Al matrix, utilizing two-beam diffraction conditions. Centered dark field images of the Al_3Zr dispersoids were formed using a $\vec{g}$ = (200) $L1_2$ superlattice reflection by tilting the incident illumination by an angle equal to the diffraction angle. To determine the particle volume fraction, the thickness of the TEM foils was measured using an Electro Energy Loss Spectroscopy (EELS) attached in the TEM. The average radius, number density and volume fraction of the dispersoids were quantified by image analysis of digitized TEM dark field images. 10 different areas (1.15 × 1.15 μm^2 for each) in the dendrite center and more than 200 particles were measured for each homogenization condition.

To quantify the recrystallized structures, all annealed samples were sectioned and polished parallel to the compression axis along the centerline and then examined using the electron backscattered diffraction (EBSD) technique under an SEM (JEOL JSM-6480LV). The surface scanning area of 0.8 mm^2 with a scanning step size of 3 μm and 3 areas at the center of each sample were selected for the recrystallization analysis.

3. Results and discussion

3.1 Precipitation behavior of Al_3Zr dispersoids during homogenization

The study of the precipitation of the Al_3Zr dispersoids during homogenization was focused on Alloy C (0.09% Zr). Typical TEM dark field images of the dispersoid precipitation after both one-step and two-step homogenization treatments are presented in Fig. 1. The corresponding selected area diffraction (SAD) pattern, as shown in the inset of Fig. 1a, indicated that the precipitates were Al_3Zr with a L12 crystal structure. Compared with the one-step homogenization, both a finer particle size and a higher number density of Al_3Zr dispersoids are obtained for all two-step homogenization conditions. The average radius, number density and volume fraction of dispersoids are listed in Table 3. It can be seen from Fig. 1 and Table 3 that the two-step homogenization with first step held at 300 ˚C has the most significant impact on the precipitation of Al_3Zr dispersoids, resulting in the finest particle size and densest distribution of dispersoids (Fig. 1b and c). Results of two holding times (48 and 72 h) are quite similar, and the dispersoid size and number density change only slightly when the holding time is prolonged from 48 to 72 h at 300 ˚C. On the other hand, the two-step homogenization with the first step treated at 400 ˚C (Fig. 1d and f) also results in a considerable reduction of dispersoid size (14 nm vs. 20.6 nm of the one-step homogenization). However, prolonging the holding time from 48 to 72 h at 400 ˚C causes a slight increase in particle size and a minor decrease in the number density of dispersoids. With respect to the volume fraction of dispersoids, the values of the volume fraction are nearly constant for all homogenization conditions, indicating that all supersaturated Zr solutes are out of the solution to form dispersoids and the volume fraction of Al_3Zr dispersoids reaches its equilibrium value after both one-step and two-step treatments.

Fig. 2 shows TEM dark field images of Al_3Zr precipitation with the first step held at 300 ˚C. After being held for 48 h, some fine dispersoids can be observed but the number of the dispersoids seems to be much smaller than that after the two-step homogenization (Fig. 2a vs. Fig. 1b). By careful observation at high magnification (Fig. 2b), it is found that, apart from relatively large dispersoids, many small dispersoid with a diameter of approximately 1-3 nm also

appeared in the aluminum matrix. Those small dispersoids are marked with arrows and their quantities are few times larger than the relatively large dispersoids. It should be mentioned that the conventional TEM used in this study has a difficulty in clearly revealing the dispersoids smaller than 1-1.5 nm. It is reasonable to believe that there are a certain number of smaller dispersoids that could not fully be revealed. It is evident that the first step treatment at 300 ˚C promotes the nucleation of a large number of dispersoids out of the aluminum matrix due to a high Zr supersaturation at low temperature. Many of those small dispersoids can only slowly grow because of the low diffusion rate of Zr atoms at low temperature of 300 ˚C (6.34×10^{-24} m^2s^{-1}). The diffusion rate of Zr in Al matrix at a given temperature is calculated from $D = D_0 \exp\left(\frac{-Q}{RT}\right)$, where $D_0 = 7.28 \times 10^{-2}$ m^2s^{-1} and $Q = 242$ kJ mol^{-1} [10]. The diffusion rates of Zr in Al matrix at the studied temperatures of 300, 400 and 470 ºC are 6.34×10^{-24}, 1.20×10^{-20} and 7.07×10^{-19} m^2s^{-1}, respectively.

After the first step treated at 400 ˚C, the number of dispersoids is clearly increased relative to the one-step homogenization. The precipitates are also verified being Al_3Zr by the SAD pattern, as presented in the inset of Fig. 3a. However, all Al_3Zr dispersoids already grow to a relatively large size (Fig. 3a) due to a high diffusion rate of Zr at 400 ˚C (1.20×10^{-20} m^2s^{-1}), and it is difficult to find small dispersoids between the existing ones (Fig. 3b). The number of dispersoids observed after first step treated at 400 ˚C is almost identical to that after the completed two-step treatment.

During homogenization, there are two main factors influencing the dispersoid precipitation: (1) the supersaturation of the solid solution (driving force for nucleation) and (2) the diffusivity of the solute in the matrix (for growth and coarsening). When treated at the high temperature of the conventional one-step practice, fewer dispersoids can form due to a low supersaturation of Zr in solid solution but they grow faster and may also coarsen because of the high diffusion rate of Zr solutes at 470 ˚C (7.07×10^{-19} m^2s^{-1}). Compared with the one-step homogenization, the driving force for dispersoid nucleation by the first step treated at lower temperatures is considerably higher because the Zr supersaturation is largely increased at lower temperature.

Therefore, a larger number dispersoids can be formed by the first step treatment. Moreover, the lower the temperature at the first step, the higher of the driving force for the nucleation but the lower of the growth rate of dispersoids are. The first step treatment at 300 ˚C produced more Al_3Zr nuclei than that at 400 ˚C. However, those small dispersoids can only slowly grow at this temperature. The subsequent second step treatment provides a normal condition for their growth. Overall, as shown in Table 3, much denser and finer dispersoids were obtained when the first step temperature was reduced from 400 to 300 ˚C.

The precipitate free zone (PFZ) of Al_3Zr dispersoids in the dendrite grain boundary can be clearly observed after one-step homogenization at 470 ˚C (Fig. 4a). Having a solid-liquid partition coefficient, k_0 = 2.5, large than unity, Zr as a peritectic element segregates inversely from the dendrite center to the interdentritic boundary during solidification, resulting in solute-rich dendritic cores surrounded by solute-depleted interdendritic region. Therefore, the precipitation of Al_3Zr dispersoids principally occurs in the dendrite cores and the particle free zone (PFZ) of Al_3Zr dispersoids forms near the interdendritic gain boundary during homogenization. The widths of PFZ are in the range of 2 to 3 μm and the distribution of dispersoids near PFZ is non-uniform. Close to the boundary, only few dispersoids with large interparticle space can be seen. Towards the dendrite center, the number of dispersoids is increased and their distribution becomes more homogeneous, which is consistent with previous studies [14, 22]. Compared with the one-step homogenization, the widths of PFZ after two-step homogenization with first step treated at 300 ˚C are reduced from 2-3 μm to 1-1.5 μm. Moreover, the number of dispersoids close to the boundary increases significantly and the size of the dispersoids decreases remarkably (Fig. 4b).

During non-equilibrium solidification, the local Zr concentration gradually decreases from the dendrite center to the boundary [8]. The one-step homogenization at a relatively high temperature (470 ˚C) results in an insufficient Zr supersaturation close to the boundary for the dispersoid precipitation. With the first step treated at lower temperature, the Zr supersaturation in the same region is increased and hence the driving force for the nucleation of the dispersoids is

significantly enhanced. Therefore, a larger number of dispersoids can be formed near the dendrite grain boundary, leading to a narrow PFZ and a dense distribution of dispersoids after two-step homogenization.

3.2 Effect of Zr contents and homogenization treatments on recrystallization resistance

In the 7xxx wrought alloys, recrystallization during post-deformation heat treatments could considerably deteriorate the alloy strength and fracture toughness. To study the effect of Zr on the recrystallization behavior of the 7150 alloys during post-deformation heat treatments, hot-deformed samples were isothermally annealed at 470 ˚C for 2 hours and subsequently water-quenched. The influence of the Zr contents on the recrystallization with the one-step homogenization is shown in Fig. 5. Samples with Zr contents from 0 to 0.09% show all partially recrystallized microstructures after annealing, and the sample with 0.16% Zr exhibits a main recovery microstructure with few, small and isolated recrystallized grains. During annealing, recrystallized grains with high-angle boundaries (>15°) were developed in those alloys, indicating the occurrence of static recrystallization. The volume fraction and average size of the recrystallized grains were quantitatively analyzed using the EBSD technique, and the results are plotted in Fig. 6. The determination of statically recrystallized grains is based on two criteria [23]: (1) the misorientation of the boundary between the recrystallized grain and the deformed matrix is larger than 15º; and (2) the mean misorientation within the recrystallized grain is lower than 1º. As shown in Fig. 6, the volume fraction and average grain size of recrystallized grain decrease with increasing Zr content. The recrystallized fraction decreases from 75% of Alloy A (base alloy without Zr) down to 1% of Alloy D (0.16% Zr), indicating a significant increase in recrystallization resistance when Zr content increases.

The microstructure evolution of Alloy B (0.04% Zr) subject to two-step homogenization treatments is shown in Fig. 7. All samples are partially recrystallized after annealing. The measured recrystallized fraction and grain size for both one-step and two-step homogenization treatments are shown in Fig. 8. Compared with the sample with the one-step homogenization, the

recrystallized fractions of the two-step homogenization samples are generally reduced, indicating a clear increase in the recrystallization resistance of the samples with two-step homogenization treatments. Moreover, the samples with the first step treated at 300 ˚C show more obvious effects that treated at 400 ˚C. Both the recrystallized fraction and grain size with first step treated at 300 ˚C are remarkably reduced relative to the one-step homogenization sample. Results also show that the holding time for the 300 ˚C and 400 ˚C conditions has a negligible impact on recrystallized fraction and grain size of recrystallization grains.

The microstructure evolution of Alloy C (0.09% Zr) with the two-step homogenization treatments is shown in Fig. 9. When the samples are subject to two-step homogenization treatments, their microstructure becomes a main recovery structure with few isolated recrystallized grains emerging. Compared with the sample subject to the one-step homogenization that is partially recrystallized (Fig. 5c), the recrystallization process is almost inhibited with two-step homogenization treatments. The measured recrystallized fraction and grain size are also displayed in Fig. 9. The recrystallized fraction and grain size are reduced to approximately 2% and 25 μm, respectively, for both first steps treated at 300 ˚C and 400 ˚C. For the sample of Alloy C (0.16% Zr), the recrystallization resistance of the alloy is already very high with the one-step homogenization and the recrystallized fraction is only approximately 1% (Fig. 5d and Fig. 6). Therefore, no two-step homogenization treatments were applied.

Coherent Al_3Zr dispersoids are known to effectively prevent the motion of subgrain boundaries during annealing, hence retarding the static recrystallization process. The effectiveness of dispersoids in preventing recrystallization can be quantified by calculating the Zener pinning pressure, P_Z, in the following equation [6, 24, 25]:

$$P_Z = \frac{3\gamma_{GB}}{2}(f/r) \quad (1)$$

where γ_{GB} is the specific grain boundary energy, f is the volume fraction and r is the average radius of dispersoids. Eq. 1 indicates that a high volume fraction of small dispersoids (*i.e.*, a high f/r value) is necessary to achieve a high P_Z on grain boundary migration for

retarding the growth of recrystallized grains. P_Z can be greatly increased by maximizing the volume fraction (f) and minimizing the dispersoid size (r). Compared with the one-step homogenization, higher f/r values of Al_3Zr dispersoids are obtained when two-step homogenization treatments are applied (Table 3), particularly for the first step treated at low temperature (300 ˚C). The f/r value increases from 0.16 of the one-step homogenization sample to 0.32 of the two-step homogenization samples with first step treated at 300 ˚C. In the alloys subject to two-step homogenization treatments, a great number of fine Al_3Zr dispersoids dispersed in the aluminum matrix, and they played a major role in inhibiting recrystallization. On the other hand, the recrystallization often occurs near dendrite grain boundaries where few dispersoids are present and the PFZ locates (a low local f/r value). The two-step homogenization treatment can reduce the width of PFZ and increase the number of dispersoids near dendrite grain boundaries (Fig. 4), leading to a high local f/r value and hence an increased P_Z in the region. As a consequence, samples subject to two-step homogenization treatments display a remarkably high recrystallization resistance. The highest recrystallization resistance is obtained when first step treated at 300 ˚C due to the highest number density and finest size of dispersoids.

4. Conclusions

(1) The conventional one-step homogenization used for the 7150 alloy produced a low number density and non-uniform distribution of Al_3Zr dispersoids. Compared with the one-step homogenization treatment, both a finer particle size and a higher number density of Al_3Zr dispersoids were obtained with the two-step homogenization treatments. When the first step was treating at 300 and 400 ˚C, the number density of dispersoids increased by 7-8 and 3-3.5 times, respectively. The most effective dispersoid distribution was attained using the first step held at 300 ˚C.

(2) The two-step homogenization treatment minimized the precipitate free zones and greatly increased the number density of dispersoids near dendrite grain boundaries, leading to a

significant improvement of dispersoid distribution in aluminum matrix.

(3) The improved dispersoid distribution through the two-step homogenization treatments can effectively inhibit the recrystallization process during post-deformation annealing for 7150 alloys containing 0.04-0.09% Zr. Compared with the one-step homogenization, both volume fraction and grain size of recrystallization grains with two-step homogenization treatments were remarkably reduced. The first step treated at low temperature (300 ˚C) was found to be mostly effective to increase the recrystallization resistance.

Acknowledgments

The authors would like to acknowledge the financial support from the Natural Sciences and Engineering Research Council of Canada (NSERC) and from Rio Tinto Alcan through the NSERC Industrial Research Chair in Metallurgy of Aluminum Transformation at the University of Québec at Chicoutimi. The authors would also like to thank Dr. Z. Zhang for his help in TEM observation.

References

[1] Immarigeon JP, Holt RT, Koul AK, Zhao L, Wallace W, Beddoes JC. Light weight materials for aircraft applications. Mater Charact 1995; 35:41-67.

[2] Heinz A, Haszler A, Keidel C, Moldenhauer S, Benedictus R, Miller WS. Recent development in aluminium alloys for aerospace applications. Mat Sci Eng A 2000; 280:102-107.

[3] Williams JC, Starke EA. Progress in structural materials for aerospace systems. Acta Mater 2003; 51:5775-5799.

[4] Starke EA, Staley JT. Application of modern aluminum alloys to aircraft. Prog Aerosp Sci 1996; 32:131-172.

[5] Ocenasek V, Slamova M. Resistance to recrystallization due to Sc and Zr addition to Al–Mg alloys. Mater Charact 2001; 47:157-162.

[6] Humphreys FJ, Hatherly M. Recrystallization and Related Annealing Phenomena, 3rd ed., Elsevier science Inc., Oxford, 1995.

[7] Knipling KE, Dunand DC, Seidman DN. Nucleation and Precipitation Strengthening in Dilute Al-Ti and Al-Zr Alloys. Metall Mater Trans A 2007; 38:2552-2563.

[8] Knipling KE, Dunand DC, Seidman DN. Precipitation evolution in Al-Zr and Al-Zr-Ti alloys during isothermal aging at 375-425 oC. Acta Mater 2008; 56:114-127.

[9] Knipling KE, Dunand DC, Seidman DN. Ambient- and high-temperature mechanical properties of isochronally aged Al-0.06Sc, Al-0.06Zr and Al-0.06Sc-0.06Zr (at.%) alloys.

Acta Mater 2011; 59:943-954.

[10] Clouet E, Sanchez JM, Sigli C. First-principles study of the solubility of Zr in Al. Phys Rev B 2002; 65:094105.

[11] Schobel M, Pongratz P, Degischer HP. Coherency loss of Al3(Sc,Zr) precipitates by deformation of an Al-Zn-Mg alloy. Acta Mater 2012; 60:4247-4254.

[12] Robson JD. Optimizing the homogenization of zirconium containing commercial aluminium alloys using a novel process model. Mater Sci Eng A 2002; 338:219-229.

[13] Jia ZH, Hu GH, Forbord B, Solberg JK. Effect of homogenization and alloying elements on recrystallization resistance of Al-Zr-Mn alloys. Mater Sci Eng A 2007; 444:284-290.

[14] Robson JD, Prangnell PB. Predicting recrystallised volume fraction in aluminium alloy 7050 hot rolled plate. Mater Sci Tech 2002;18:607-614.

[15] Deng YL, Wan L, Wu LH, Zhang YY, Zhang XM. Microstructural evolution of Al-Zn-Mg-Cu alloy during homogenization. J Mater Sci 2011; 46:875-881.

[16] Morere B, Shahani R, Maurice C, Driver J. The influence of Al3Zr dispersoids on the recrystallization of hot-deformed AA 7010 alloys. Metall Mater Trans A 2001; 32:625-632.

[17] Robson JD, Prangnell PB. Modelling Al3Zr dispersoid precipitation in multicomponent aluminium alloys. Mater Sci Eng A 2003; 352:240-250.

[18] Eivani AR, Ahmed H, Zhou J, Duszczyk J. An experimental and theoretical investigation of the formation of Zr-containing dispersoids in Al-4.5Zn-1Mg aluminum alloy. Mater Sci Eng A 2010; 527:2418-2430.

[19] Jia ZH, Hu GH, Forbord B, Solberg JK. Enhancement of recrystallization resistance of Al-Zr-Mn by two-step precipitation annealing. Mater Sci Eng A 2008; 483-484:195-198.

[20] Lu XY, Guo EJ, Rometsch P, Wang LJ. Effect of one-step and two-step homogenization treatments on distribution of Al3Zr dispersoids in commercial AA7150 aluminium alloy. T Nonferr Metal Soc 2012; 22:2645-2651.

[21] Ou BL, Yang JG, Wei MY.Effect of Homogenization and Aging Treatment on Mechanical Properties and Stress-Corrosion Cracking of 7050 Alloys. Metall Mater Trans A 2007;

38:1760-1773.

[22] Deng YL, Zhang YY, Wan L, Zhu AA, Zhang XM. Three-Stage Homogenization of Al-Zn-Mg-Cu Alloys Containing Trace Zr. Metall Mater Trans A 2013; 44:2470-2477.

[23] Humphreys FJ. Review-Grain and subgrain characterisation by electron backscatter diffraction. J Mater Sci 2001; 36:3833-3854.

[24] Nes E, Ryum N, Hunderi O. On the Zener drag. Acta Met Mater 1985; 33:11-22.

[25] Doherty RD. Role of interfaces in kinetics of internal shape changes. Mater Sci 1982; 16:1-13.

Tables

Table 1
Chemical compositions of experimental alloys (wt%)

Alloys	Zn	Mg	Cu	Zr	Fe	Si	Ti	Al
A (base)	6.15	2.10	2.11	0	0.13	0.11	0.008	Bal.
B	6.10	2.00	2.15	0.04	0.13	0.11	0.008	Bal.
C	5.99	1.91	2.10	0.09	0.13	0.11	0.008	Bal.
D	6.00	2.08	2.09	0.16	0.13	0.12	0.008	Bal.

Table 2
Temperature and time of one-step and two-step homogenization treatments applied

Heat Treatment	First step		Second step	
	Temperature (°C)	Time (h)	Temperature (°C)	Time (h)
One-step	—	—	470	24
Two-step	300	48	470	24
	300	72	470	24
	400	48	470	24
	400	72	470	24

Table 3
Average radius, number density and volume fraction of Al_3Zr dispersoids in 7150-0.09Zr alloy after homogenization treatments.

Homogenization conditions	Homogenization parameters	Average radius r (nm)	Number density N (μm^{-3})	Volume fraction f (%)	f / r (μm^{-1})
One-step	470 °C /24h	20.6	85	0.342	0.164
Two-step	300 °C /48h＋470 °C /24h	10.7	629	0.338	0.314
	300 °C /72h＋470 °C /24h	10.3	673	0.333	0.323
	400 °C /48h＋470 °C /24h	13.4	290	0.332	0.248
	400 °C /72h＋470 °C /24h	13.9	279	0.339	0.243

Figures

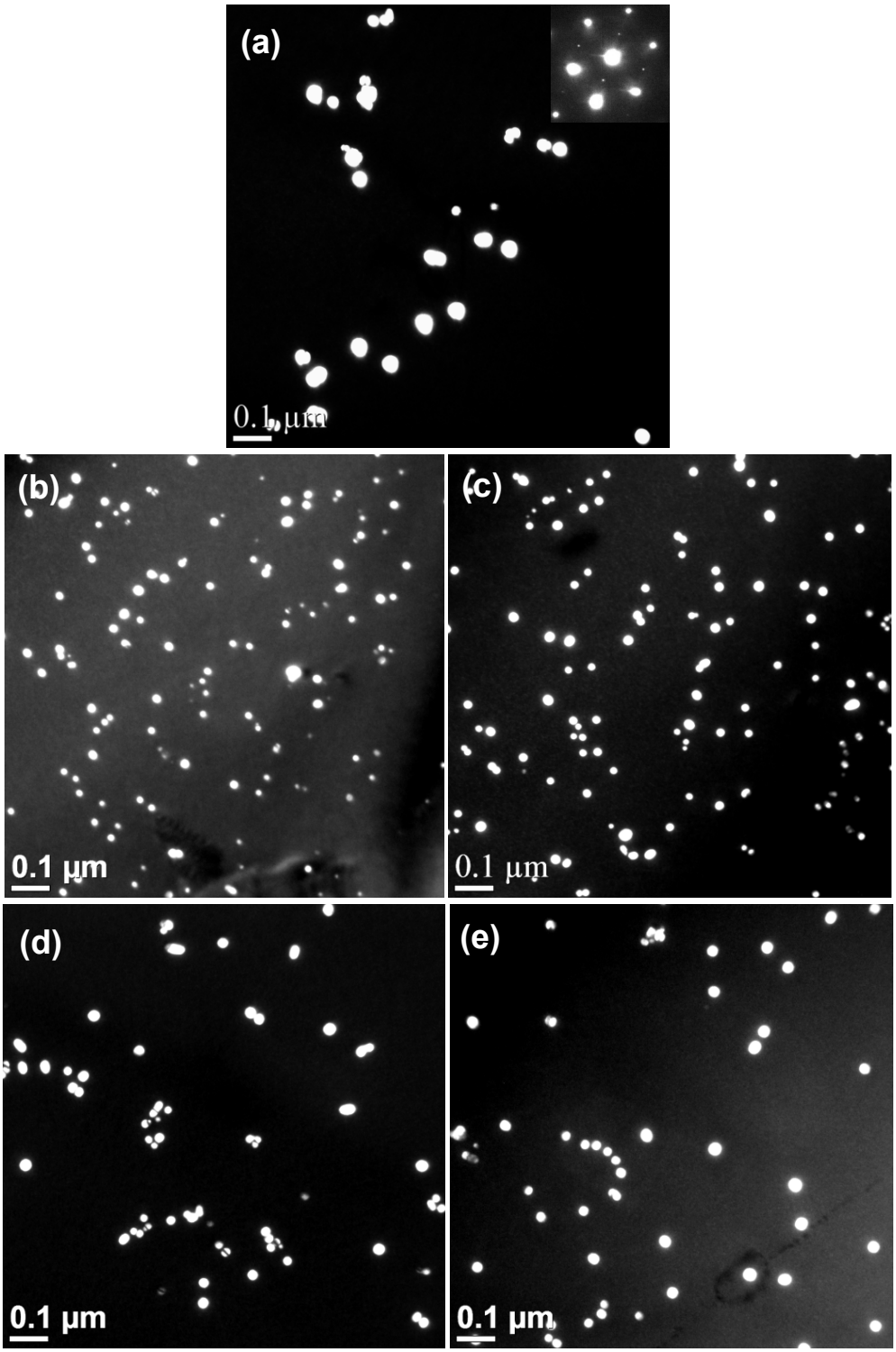

Fig. 1. Typical TEM centered dark field images of Al_3Zr dispersoids in 7150-0.09Zr alloy after both one-step and two-step homogenization treatments:
(a) 470 °C/24h with an inset of SAD pattern, (b) 300 °C/48h＋470 °C /24h, (c) 300 °C /72h＋470 °C /24h, (d) 400 °C /48h＋470 °C /24h, and (e) 400 °C /72h＋470 °C /24h.

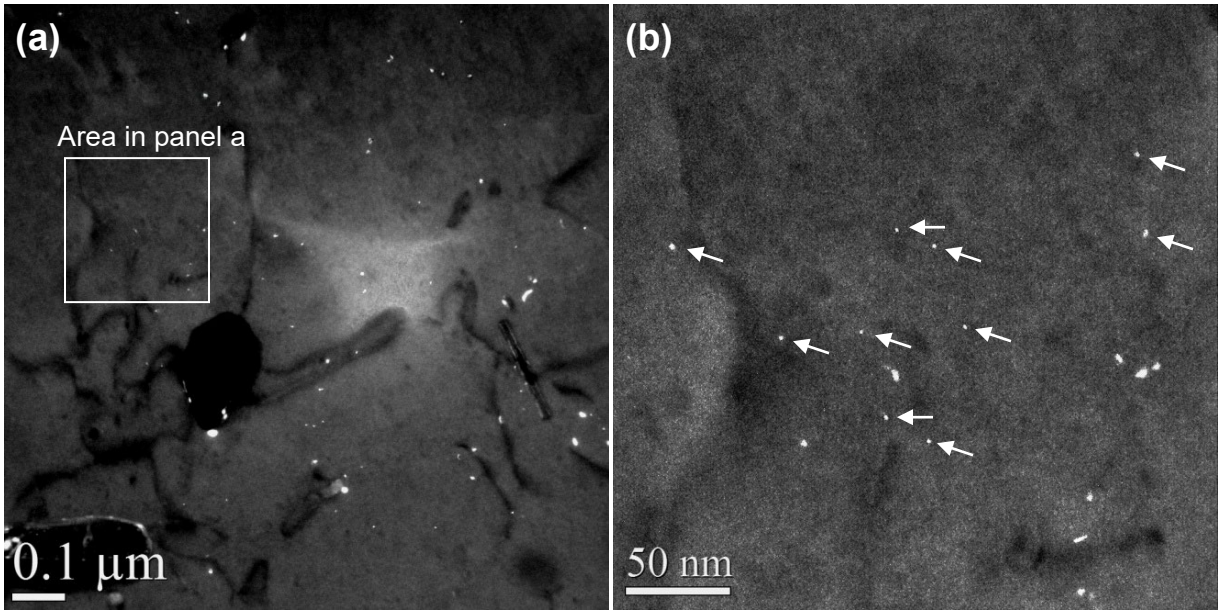

Fig. 2. TEM centered dark field images of Al_3Zr dispersoid precipitate after the first step homogenization treated at: (a) 300 ^oC for 48h, and (b) magnified area a.

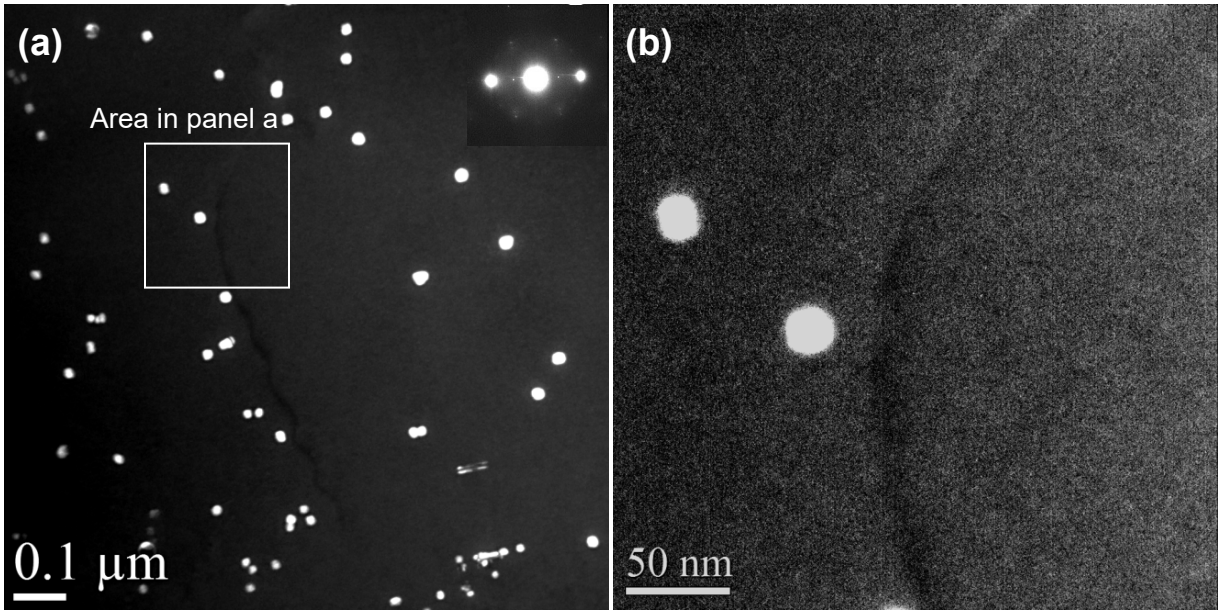

Fig. 3. TEM centered dark field images of Al_3Zr dispersoid precipitate after the first step homogenization treated at: (a) 400 ^oC for 48h with an inset of SAD pattern, and (b) magnified area a.

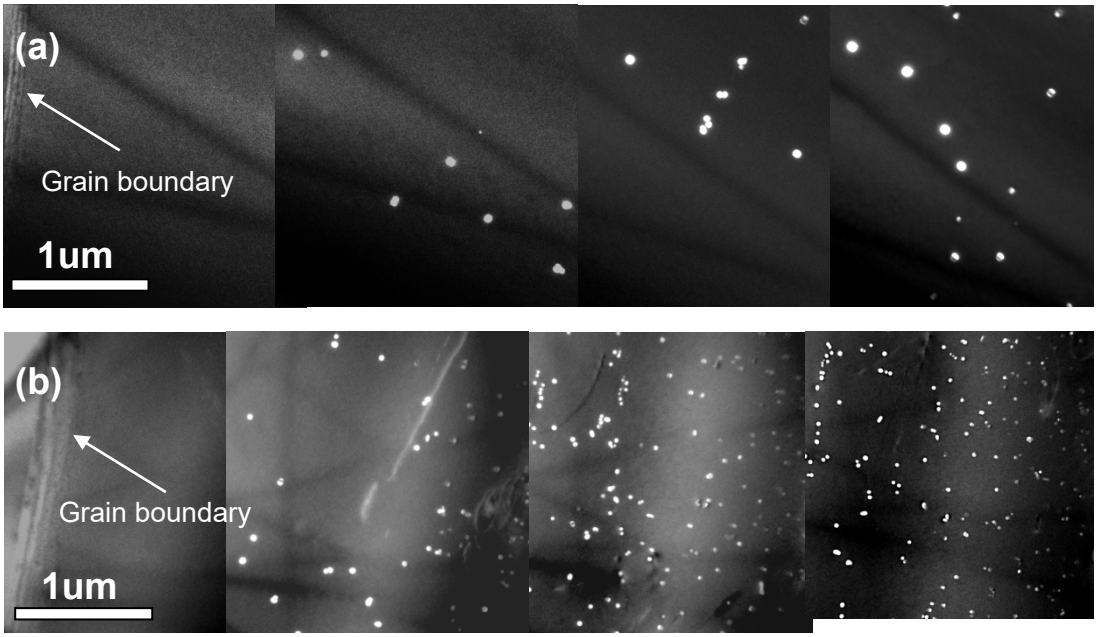

Fig. 4. TEM dark field images of the distribution of Al_3Zr dispersoids in grain boundary regions of subjected to different homogenization treatments:
(a) one-step, 470 ºC × 24h, (b) two-step, 300 ºC × 48h + 470 ºC × 24h.

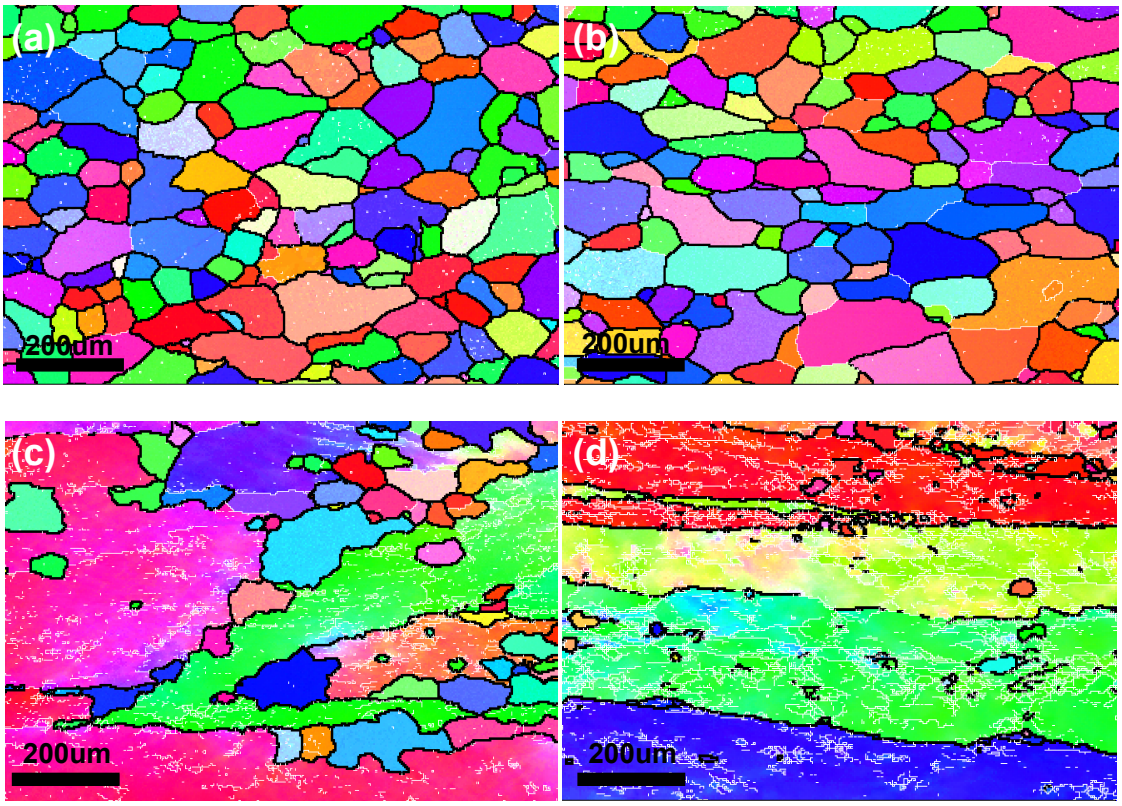

Fig. 5. Orientation maps of 7150 alloys with different Zr contents subject to one-step homogenization: (a) the base alloy (0% Zr); (b) 0.04 Zr %; (c) 0.09Zr %; (d) 0.16Zr %. High angle grain boundaries (>15°) and low angle grain boundaries (2 - 15°) shown as black line and white line, respectively.

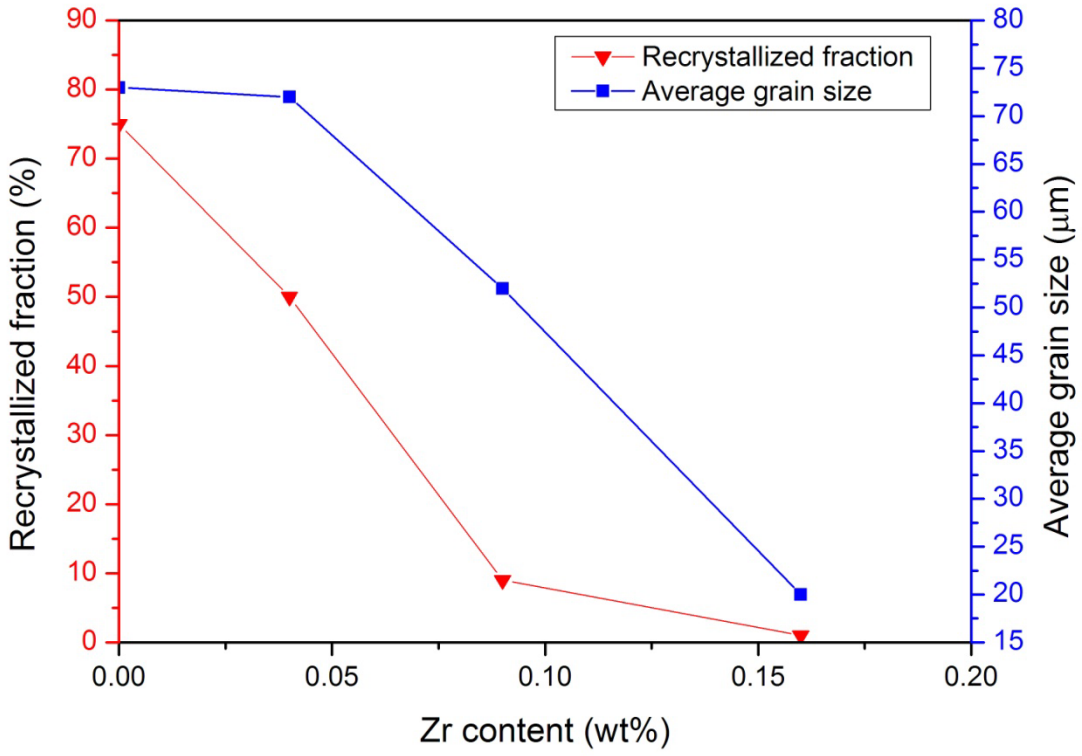

Fig. 6. Volume fraction and average size of recrystallized grains as a function of Zr contents for 7150 alloys subject to one-step homogenization.

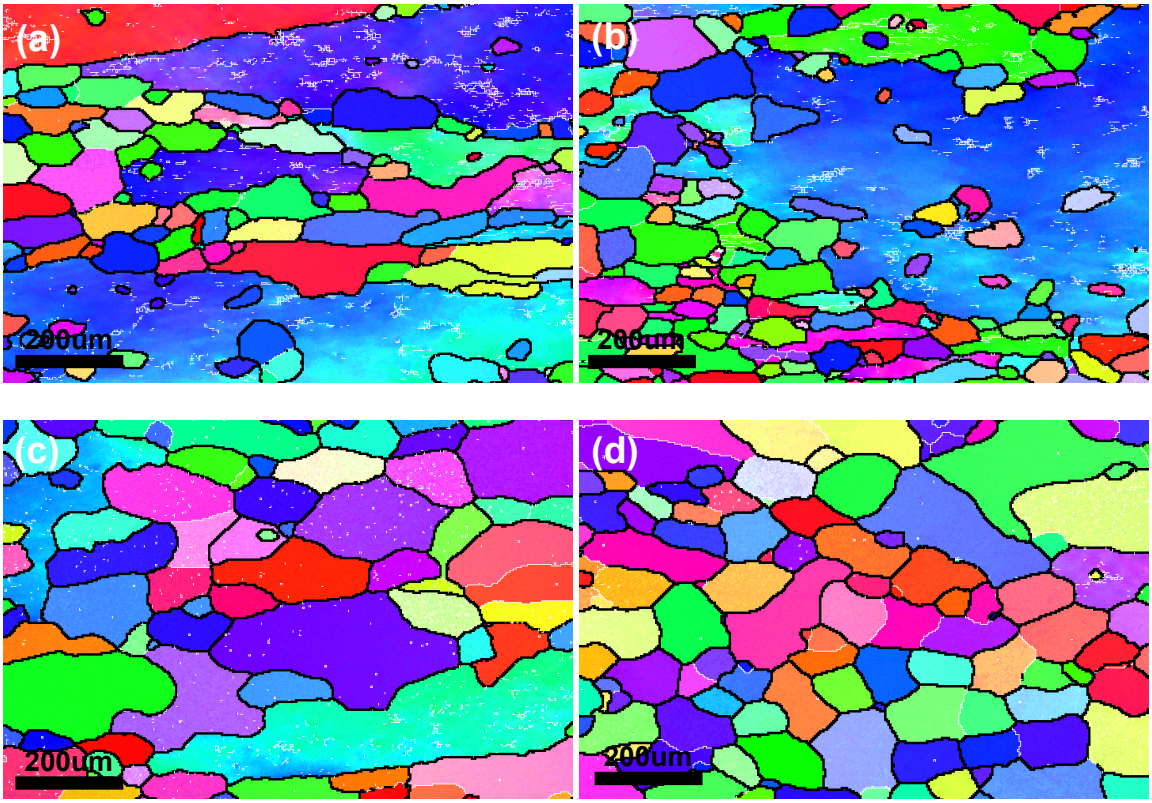

Fig. 7. Orientation maps of 7150-0.04Zr Al alloy homogenized at: (a) 300 ºC /48h＋470 ºC /24h; (b) 300 ºC /72h＋470 ºC /24h; (c) 400 ºC /48h＋470 ºC /24h; (d) 400 ºC /72h＋470 ºC /24h.

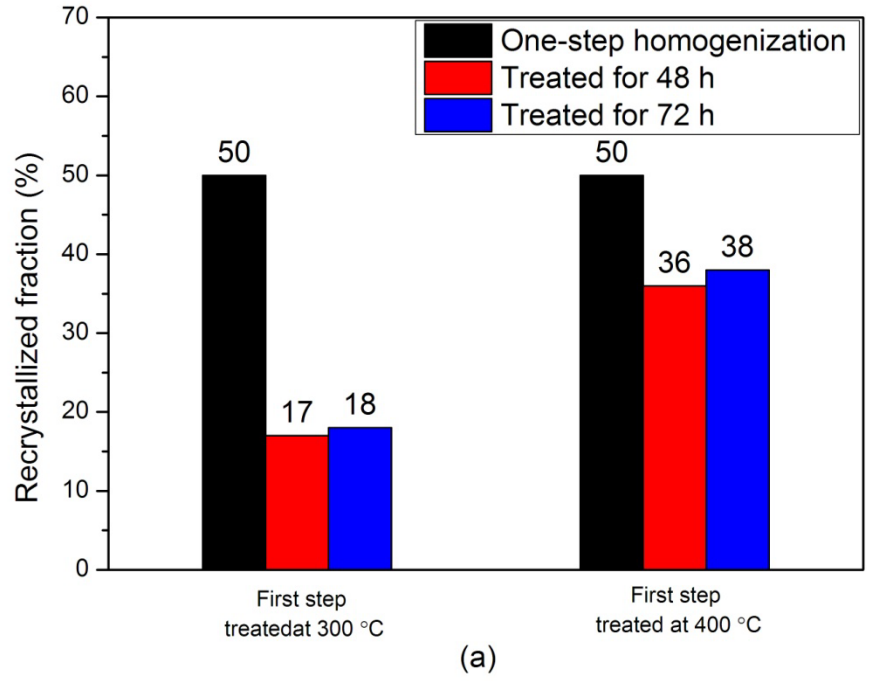

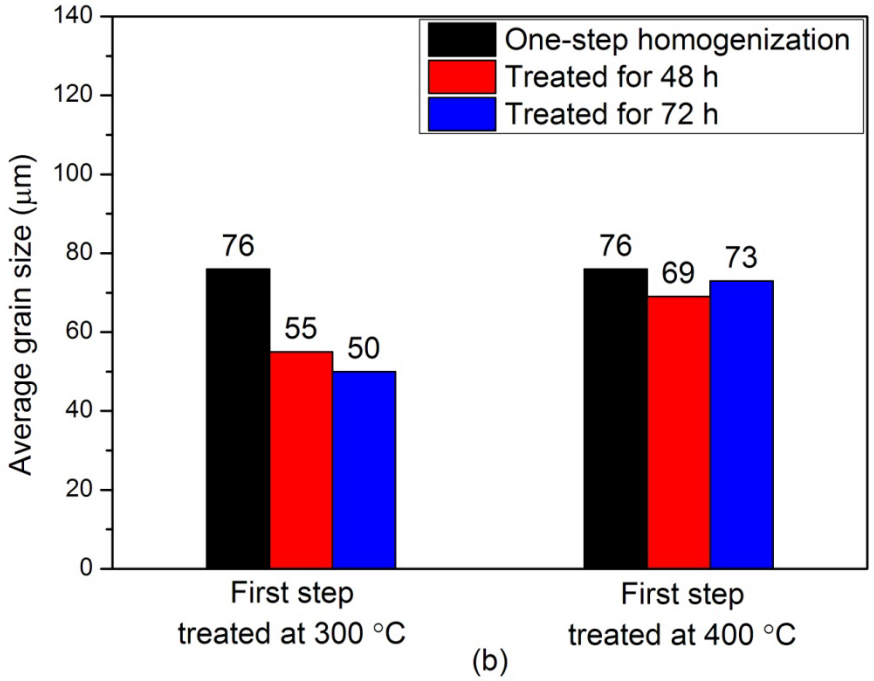

Fig. 8. Volume fraction and average size of recrystallized grain of 7150-0.04Zr alloy subject to both one-step and two-step homogenization treatments: (a)volume fraction; (b)average grain size.

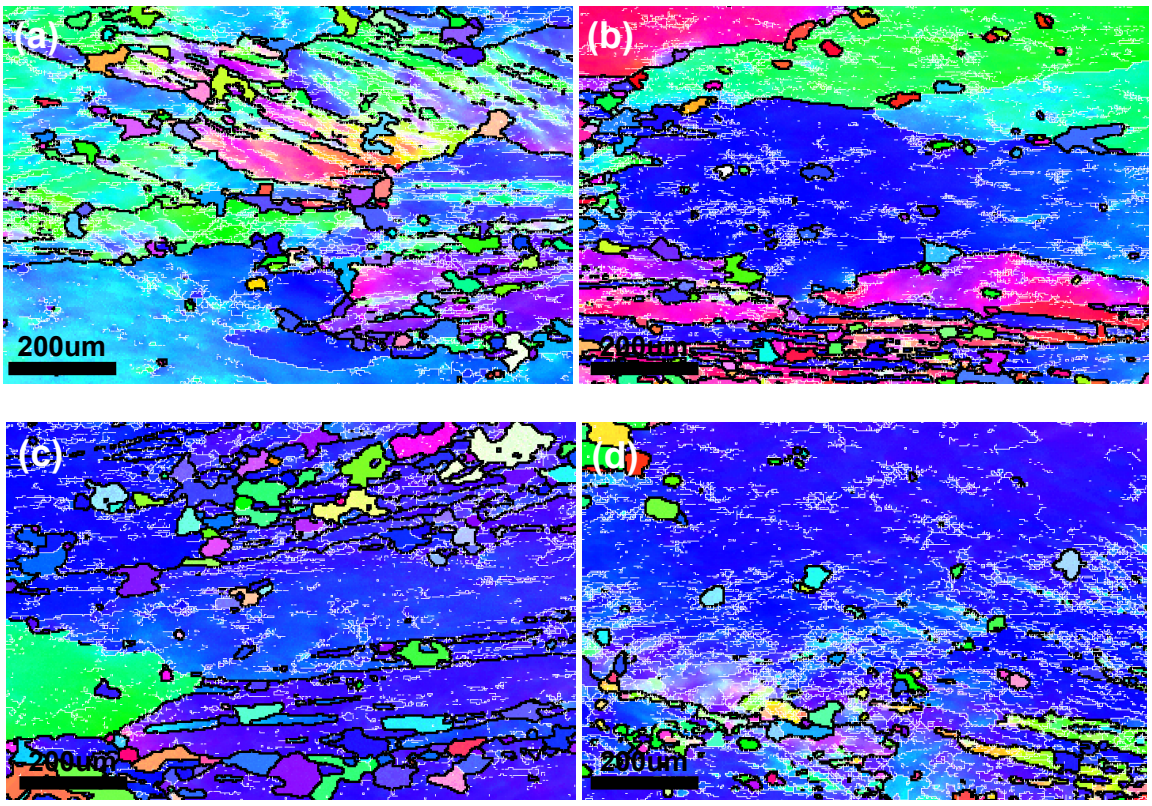

Fig. 9. Orientation maps of 7150-0.09Zr alloy homogenized at: (a) 300 ºC /48h＋470 ºC /24h; (b) 300 ºC /72h＋470 ºC /24h; (c) 400 ºC /48h＋470 ºC /24h; (d) 400 ºC /72h＋470 ºC /24h.

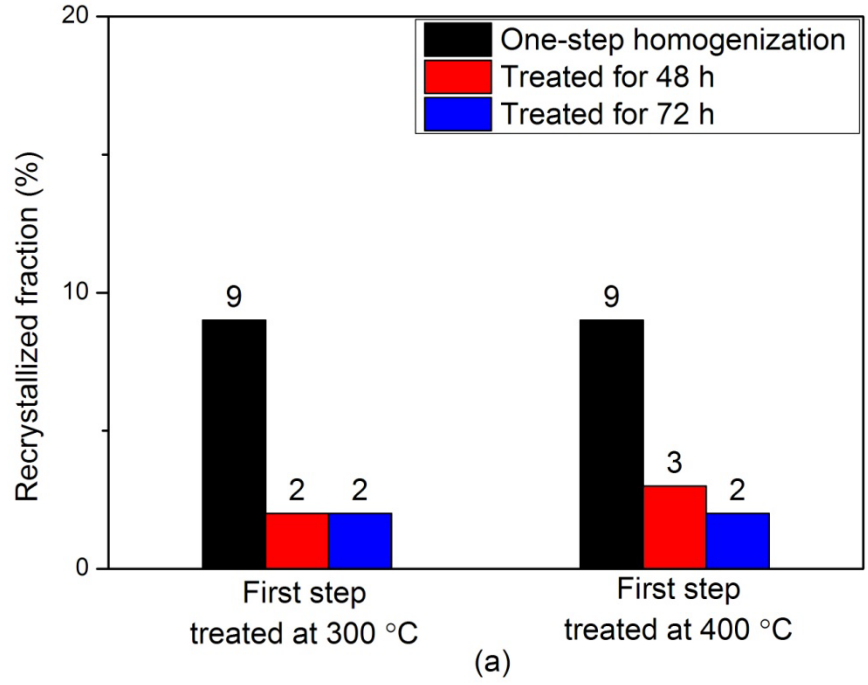

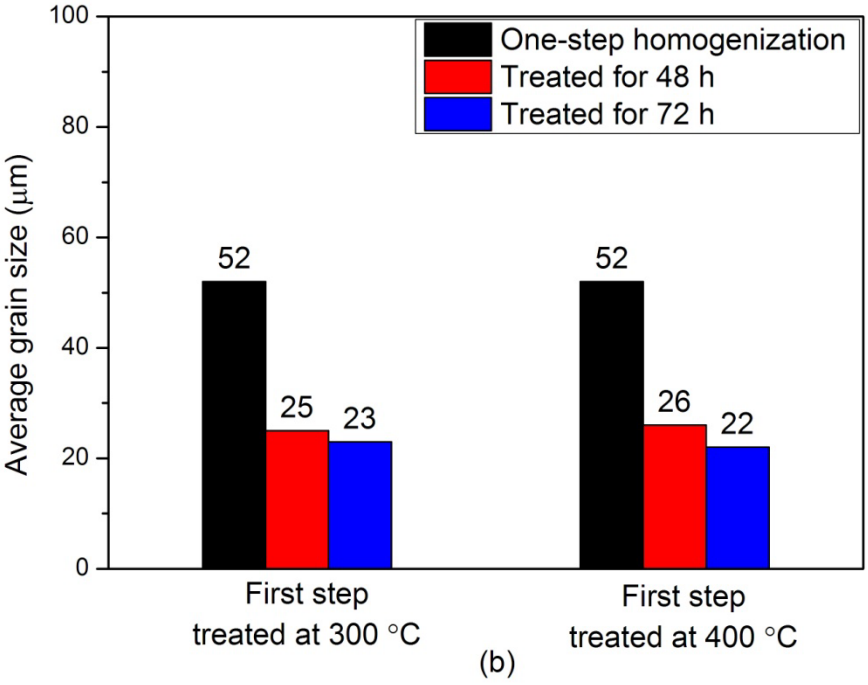

Fig. 10. volume fraction and average size of recrystallized grains of 7150-0.09Zr Al alloy subject to both one-step and two-step homogenization treatments: (a) volume fraction; (b) average grain size.